DOI: 10.1109/TSP.2015.2415754
To cite this article: A. Coluccia and G. Ricci, "ABORT-Like Detection Strategies to Combat Possible Deceptive ECM Signals in a Network of Radars," in IEEE Transactions on Signal Processing, vol. 63, no. 11, pp. 2904-2914, June 1, 2015, doi: 10.1109/TSP.2015.2415754.

ABORT-like detection strategies to combat possible deceptive ECM signals in a network of radars

Angelo Coluccia, *Member, IEEE* and Giuseppe Ricci, *Senior Member, IEEE*

***Abstract*—We address adaptive detection of coherent signals backscattered by possible point-like targets in presence of thermal noise, clutter, noise-like interferers and, possibly, coherent interferers, i.e., deceptive electronic countermeasure (ECM). To this end, we assume a network of radars: for a given cell under test only a subset of the radars receives ECM signals. Training data containing thermal noise, clutter, and noise-like interferers are available. The problem at hand is solved resorting to the generalized likelihood ratio test (GLRT) and to ad hoc solutions: at the design stage we assume that data collected by the radars can be noise only (namely, thermal noise, clutter, and possible noise-like interferers) plus possible coherent interferers or noise plus coherent useful signal. The performance assessment shows that the proposed solutions are effective in presence of ECM systems.**

***Index Terms*—Adaptive radar detection, constant false alarm rate (CFAR), generalized likelihood ratio test (GLRT), digital radio frequency memory (DRFM), electronic countermeasure (ECM), electronic counter-countermeasures (ECCM).**

I. Introduction

Electronic countermeasure (ECM) techniques are aimed at denying information (detection, position, track initiation, etc. of one or more targets) that the victim radar seeks, or at surrounding desired radar echoes with so many false targets that the true information cannot be extracted [1]. On the other hand, nowadays radar systems are equipped with the so-called electronic counter-countermeasures (ECCM) which are aimed at countering the effects of the enemy's ECM and eventually succeeding in the intended mission. ECCM techniques can be categorized as antenna-based, transmitter-based, receiver-based, and signal-processing-based depending on the main radar subsystem where they take place. The reader is referred to [1, and references therein] for a detailed description of the major ECCM techniques.

An effective category of ECM techniques is the so-called deceptive ECM (DECM). Deception is the intentional and deliberate transmission or retransmission of amplitude, frequency, phase, or otherwise modulated intermittent or continuous wave signals for the purpose of misleading in the interpretation or use of information by the radar. In particular, repeater DECM systems generate coherent returns that attempt to emulate the amplitude, frequency, and temporal characteristics of actual radar returns. Repeaters are usually implemented using a digital radio frequency memory (DRFM) [2], [3]. In a DRFM system the input radio frequency signal is generally first down-shifted in frequency and then sampled with a high-speed analog-to-digital converter (ADC). The stored samples are manipulated in amplitude, frequency, and phase and subsequently processed by a digital-to-analog (DAC) converter, up converted, and transmitted back to the victim radar. A typical DECM technique is the range gate pull off (RGPO) aimed at introducing a false target into the radar return signal; since the deception signal is typically stronger than the radar return signal, it captures the range-tracking circuits. The deception signal is then progressively delayed using the DRFM, thereby "walking" the range gate off the actual target. When the range gate is sufficiently removed from the actual target, the deception jammer is turned off, thus forcing the radar into a target reacquisition mode [1].

Antenna-related techniques capable of preventing jamming signals from entering through the radar sidelobes are the so-called sidelobe blanking (SLB) and sidelobe canceling (SLC) techniques [4]. A SLB system is effective against interference pulses (but also strong targets) entering the radar receiver via the antenna sidelobes; in particular, it can be used to suppress coherent repeater interference (CRI). The idea is that, employing an auxiliary antenna (coupled to a parallel receiving channel) in addition to the main antenna, it is possible, by suitable choice of the antenna gains, to distinguish signals entering the sidelobes from those entering the mainlobe (and the former may be suppressed). However, the possible presence of noise-like interference (NLI) makes the detection task even more challenging. In fact, it has been shown in [4] that the presence of NLI can reduce the capability of a conventional SLB of blanking CRI. Suppression of NLI can be accomplished via a sidelobe canceler (SLC) system. SLC uses an array of auxiliary antennas to adaptively estimate the direction of arrival and the power of the jammers and, subsequently, to modify the receiving pattern of the radar antenna placing nulls in the jammers' directions. Since SLB is effective against CRI whereas SLC combats (continuous) NLI, SLB and SLC can be jointly used against their simultaneous presence [5]. In [4] it is also shown that a data dependent threshold (DDT), based on [6], outperforms a cascade of SLC and SLB stages. The important result is that the DDT should be preferred to the latter because, with the same number of receiving channels, it allows to cancel one more NLI.

The detector proposed in [6] is a special case of the more general class of tunable (possibly space-time) detectors which

A. Coluccia and G. Ricci are with the Dipartimento di Ingegneria dell'Innovazione, Università del Salento, Via Monteroni, 73100 Lecce, Italy. Phone: +39 0832 297205. Fax: +39 0832 325362. E-Mail: [angelo.coluccia, giuseppe.ricci]@unisalento.it.

have been shown to be an effective means to attack detection of mainlobe targets or rejection of CRI notwithstanding the presence of NLI and clutter [6]-[18]. A way to design tunable receivers relies on the so-called two-stage architecture; such schemes are formed by cascading two detectors (usually with opposite behaviors in terms of selectivity): the overall one declares the presence of a target in the cell under test only when data survive both detection thresholdings [7]-[10], [14]-[18]. Such detectors can also be used as classifiers: in this case, the first stage is less selective than the second one and it is used to discriminate between the null hypothesis and the alternative that a structured signal is present. In case of detection, the second stage is aimed at discrimination between mainlobe and sidelobe signals, as explicitly shown in [15] for the adaptive sidelobe blanker (ASB) (referred to in the following as the modified ASB in order to stress its classification capabilities). Adaptive detection and discrimination between useful signals and CRI in presence of thermal noise, clutter, and possible NLI has also been addressed in [19]. To this end, a class of detectors is proposed by resorting to a generalized likelihood ratio test (GLRT)-based for multiple hypotheses [20]. In particular, therein the CRI is assumed to belong to the orthogonal complement of the space spanned by the nominal steering vector (after whitening by the true covariance matrix of the composite disturbance). This approach, based on a modified adaptive beamformer orthogonal rejection test (ABORT), see also [18], [21], allows to investigate the discrimination capabilities of adaptive arrays when the CRI is not necessarily confined to the "sidelobe beam pattern," but might also be a mainlobe deception jammer.

It is also worth noting that most of the above adaptive detectors guarantee the constant false alarm rate (CFAR) property. Adaptive CFAR detectors are really ECCM techniques (of the signal-processing-related category) since they enhance the detection against structured interferences (in space and/or time) while maintaining the CFAR property that allows these detected targets to be effectively tracked.

In this paper, we assume a network of radars: for a given cell under test only a subset of the radars receives ECM signals (CRI). This means that space diversity can be exploited, in addition to other differences between the signature of the target and the CRI. The problem at hand is solved resorting to the GLRT and to ad hoc solutions. At the design stage we assume that data collected by the radars can be noise only (namely, thermal noise, clutter, and NLI) plus possible CRI or noise plus a coherent useful signal. More precisely, we consider two different instances: the subset of radars under ECM is preassigned (i.e., deterministically given, but not necessarily known) as in [22], or each radar is under ECM with a given probability. The remainder of the paper is organized as follows: next section is devoted to the problem formulation and to the description of the newly-proposed detectors. Section III provides the performance assessment of the detectors (also in comparison to natural competitors). Concluding remarks are given in Section IV while Appendix A contains some mathematical derivations.

II. Problem Statement and Detector Designs

Assume that a network of N_R radars senses the surveillance area. Each radar is equipped with a linear array formed by N_a antennas that collect N_t samples from the range cell under test (CUT). The signal received from the CUT can be noise only, i.e., thermal noise plus clutter (including possible NLI) or a noisy version of the signal backscattered by the target that we model as a coherent target echo. The signal received from a subset of the radars and from the CUT may also contain a manipulated radar signal (a CRI). As customary, we suppose that a set of secondary data, free of signal components and CRI, but sharing the same statistical properties of the remaining disturbance in the CUT, is available (namely that each radar experiences an homogeneous environment). Secondary data are usually chosen as range cells surrounding the CUT in order to preserve the homogeneity assumption. Focusing on data collected by the ith radar, $i \in \mathcal{N}_R = \{1, \ldots, N_R\}$, we denote by $\boldsymbol{z}_i \in \mathbb{C}^{N\times 1}$, $N = N_a \times N_t$, the vector containing the returns from the CUT and by $\boldsymbol{z}_{i,k} \in \mathbb{C}^{N\times 1}$, $k = 1, \ldots, K$, $K \geq N$, the secondary data. The problem of detecting the possible presence of a coherent return from a given cell (in range, doppler, and azimuth) is formulated in terms of the following hypothesis test

$$\begin{cases} H_0 : \begin{cases} \boldsymbol{z}_i = \boldsymbol{n}_i + I_i \boldsymbol{u}_i, & i \in \mathcal{N}_{\mathcal{R}} \\ \boldsymbol{z}_{i,k} = \boldsymbol{n}_{i,k}, & i \in \mathcal{N}_{\mathcal{R}}, k = 1, \ldots, K \end{cases} \\ \\ H_1 : \begin{cases} \boldsymbol{z}_i = x_i \boldsymbol{v}_i + \boldsymbol{n}_i, & i \in \mathcal{N}_{\mathcal{R}} \\ \boldsymbol{z}_{i,k} = \boldsymbol{n}_{i,k}, & i \in \mathcal{N}_{\mathcal{R}}, k = 1, \ldots, K \end{cases} \end{cases} \tag{1}$$

where

- $\boldsymbol{v}_i \in \mathbb{C}^{N\times 1}$ is the known steering vector of the target as viewed by the ith radar.
- $\boldsymbol{u}_i \in \mathbb{C}^{N\times 1}$ is an unknown vector representing the possible presence of the CRI; it is modeled as a signal orthogonal to $\boldsymbol{v}_i$ in the whitened space [21].
- $x_i \in \mathbb{C}$ is an unknown (deterministic) factor.
- I_i is an indicator function that takes on values 0 and 1. We can either model the I_is as deterministic (known or better unknown) parameters or as random variables (rvs) with a preassigned (not necessarily known) statistical characterization; for instance, we might assume $I_1, \ldots, I_{N_R}$ to be independent and identically distributed (iid) Bernoulli rvs, $I_i \sim \mathcal{B}(1, p)$, and, in addition, suppose that the set $\{I_1, \ldots, I_{N_R}\}$ is independent of that of the noise terms. Notice that, for $N_R = 1$ and $p = 0$, the above hypothesis testing problem reduces to that leading to Kelly's detector [23]; similarly, for $N_R = 1$ and $p = 1$, the above hypothesis testing problem reduces to that leading to the whitened-ABORT (W-ABORT) [21].
- The $\boldsymbol{n}_i$ and the $\boldsymbol{n}_{i,k} \in \mathbb{C}^{N\times 1}$, $i \in \mathcal{N}_{\mathcal{R}}$, $k = 1, \ldots, K$, are iid complex normal random vectors with zero mean and unknown, positive definite covariance matrix $\boldsymbol{R}_i \in \mathbb{C}^{N\times N}$, i.e., $\boldsymbol{n}_i$, $\boldsymbol{n}_{i,k} \sim \mathcal{CN}_N(\boldsymbol{0}, \boldsymbol{R}_i)$.

It is worth remarking that $\boldsymbol{u}_i$ is introduced at the design stage to enhance the selectivity of the detector, making it more inclined to decide for H_0 in case of mismatches, i.e., when a CRI is present [21]. Clearly, although it is not required that the actual CRI is orthogonal to $\boldsymbol{v}_i$, the ability of the detector to reject mismatched signals will depend on their degree of deviation (in the whitened space) from $\boldsymbol{v}_i$. As a matter of fact, the assumption about $\boldsymbol{u}_i$ is only a way to represent what is different from $\boldsymbol{v}_i$ without adopting any specific ECM model[1].

We cannot resort to the Neyman-Pearson criterion since we do not know $x_i \in \mathbb{C}$, $\boldsymbol{R}_i \in \mathbb{C}^{N\times N}$, $\boldsymbol{u}_i \in \mathbb{C}^{N\times 1}$, and, possibly, I_i. We can resort instead to the GLRT and to ad hoc solutions.

For future reference, denote by $\boldsymbol{Z}_i$ the overall data matrix collected from the ith radar, i.e.,

$$\boldsymbol{Z}_i = [\boldsymbol{z}_i \ \boldsymbol{z}_{i,1} \ \cdots \ \boldsymbol{z}_{i,K}] \tag{2}$$

and by $f_i(\cdot)$ the density of the $\boldsymbol{n}_i$ and the $\boldsymbol{n}_{i,k}$, i.e.,

$$f_i(\boldsymbol{n}) = \frac{1}{\pi^N \det(\boldsymbol{R}_i)} \mathrm{e}^{-\boldsymbol{n}^\dagger \boldsymbol{R}_i^{-1} \boldsymbol{n}}, \quad \boldsymbol{n} \in \mathbb{C}^{N\times 1}$$

with † denoting conjugate transpose, $\det(\cdot)$ the determinant of the matrix argument, and $^{-1}$ the matrix inverse.

A. GLRT and ad hoc detector for deterministic I_i

Herein we model the I_is as deterministic parameters; moreover, we denote by $\mathcal{N}_{\mathcal{R}1} \subset \mathcal{N}_{\mathcal{R}}$ the set of integers indexing the I_is that are equal to one. Assume that $\mathcal{N}_{\mathcal{R}1}$ is known; later we will discuss how this information can be practically obtained by means of an additional pre-detection stage.

The pdf of $\boldsymbol{Z}_i$ is given by

$$\begin{aligned} f_{1,i}(\boldsymbol{Z}_i) &= f_i\left(\boldsymbol{z}_i - x_i \boldsymbol{v}_i\right) \prod_{k=1}^{K} f_i\left(\boldsymbol{z}_{i,k}\right) \\ &= \frac{1}{\pi^N \det(\boldsymbol{R}_i)} \mathrm{e}^{-\left(\boldsymbol{z}_i - x_i \boldsymbol{v}_i\right)^\dagger \boldsymbol{R}_i^{-1} \left(\boldsymbol{z}_i - x_i \boldsymbol{v}_i\right)} \\ &\times \prod_{k=1}^{K} \frac{1}{\pi^N \det(\boldsymbol{R}_i)} \mathrm{e}^{-\boldsymbol{z}_{i,k}^\dagger \boldsymbol{R}_i^{-1} \boldsymbol{z}_{i,k}} \end{aligned} \tag{3}$$

under H_1. Similarly, under H_0, the pdf of $\boldsymbol{Z}_i$ is

$$f_{0,i}(\boldsymbol{Z}_i) = \begin{cases} f_i\left(\boldsymbol{z}_i\right) \prod_{k=1}^{K} f_i\left(\boldsymbol{z}_{i,k}\right), & i \in \mathcal{N}_{\mathcal{R}} \setminus \mathcal{N}_{\mathcal{R}1} \\ f_i\left(\boldsymbol{z}_i - \boldsymbol{u}_i\right) \prod_{k=1}^{K} f_i\left(\boldsymbol{z}_{i,k}\right), & i \in \mathcal{N}_{\mathcal{R}1} \end{cases}$$

that is

$$f_{0,i}(\boldsymbol{Z}_i) = \begin{cases} \frac{1}{\pi^N \det(\boldsymbol{R}_i)} \mathrm{e}^{-\boldsymbol{z}_i^\dagger \boldsymbol{R}_i^{-1} \boldsymbol{z}_i} \\ \times \prod_{k=1}^{K} \frac{1}{\pi^N \det(\boldsymbol{R}_i)} \mathrm{e}^{-\boldsymbol{z}_{i,k}^\dagger \boldsymbol{R}_i^{-1} \boldsymbol{z}_{i,k}}, \\ \qquad i \in \mathcal{N}_{\mathcal{R}} \setminus \mathcal{N}_{\mathcal{R}1} \\ \frac{1}{\pi^N \det(\boldsymbol{R}_i)} \mathrm{e}^{-\left(\boldsymbol{z}_i - \boldsymbol{u}_i\right)^\dagger \boldsymbol{R}_i^{-1} \left(\boldsymbol{z}_i - \boldsymbol{u}_i\right)} \\ \times \prod_{k=1}^{K} \frac{1}{\pi^N \det(\boldsymbol{R}_i)} \mathrm{e}^{-\boldsymbol{z}_{i,k}^\dagger \boldsymbol{R}_i^{-1} \boldsymbol{z}_{i,k}}, \\ \qquad i \in \mathcal{N}_{\mathcal{R}1}\,. \end{cases}$$

[1]Indeed, in Section III the performance assessment does not impose any orthogonality: the CRI is simulated via a signal similar to $\boldsymbol{v}_i$, but for some Doppler mismatch aimed at deceiving the detector with a false target.

Remember that the unknown parameters are the $\boldsymbol{R}_i$s, $i \in \mathcal{N}_{\mathcal{R}}$, under both hypotheses, the $\boldsymbol{u}_i$s, $i \in \mathcal{N}_{\mathcal{R}1}$, under H_0, and the x_is, $i \in \mathcal{N}_{\mathcal{R}}$, under H_1. Then, the GLRT is

$$\prod_{i \in \mathcal{N}_{\mathcal{R}1}} \frac{\max_{x_i} \max_{\boldsymbol{R}_i} f_{1,i}\left(\boldsymbol{Z}_i\right)}{\max_{\boldsymbol{u}_i} \max_{\boldsymbol{R}_i} f_{0,i}\left(\boldsymbol{Z}_i\right)} \times \prod_{i \in \mathcal{N}_{\mathcal{R}} \setminus \mathcal{N}_{\mathcal{R}1}} \frac{\max_{x_i} \max_{\boldsymbol{R}_i} f_{1,i}\left(\boldsymbol{Z}_i\right)}{\max_{\boldsymbol{R}_i} f_{0,i}\left(\boldsymbol{Z}_i\right)} \underset{H_0}{\overset{H_1}{\gtrless}} T \tag{4}$$

where T is a threshold to be set according to the desired probability of false alarm (P_{fa}).

It is well-known that [18], [21], [23]

$$\begin{aligned} \max_{x_i, \boldsymbol{R}_i} f_{1,i}\left(\boldsymbol{Z}_i\right) &= \left(\frac{K+1}{\pi e}\right)^{(K+1)N} \frac{1}{\det^{K+1}\left(\boldsymbol{S}_i\right)} \\ &\times \frac{1}{\left(1 + \boldsymbol{z}_i^\dagger \boldsymbol{S}_i^{-1} \boldsymbol{z}_i - \frac{|\boldsymbol{z}_i^\dagger \boldsymbol{S}_i^{-1} \boldsymbol{v}_i|^2}{\boldsymbol{v}_i^\dagger \boldsymbol{S}_i^{-1} \boldsymbol{v}_i}\right)^{K+1}} \end{aligned} \tag{5}$$

where

$$\boldsymbol{S}_i = \sum_{k=1}^{K} \boldsymbol{z}_{i,k} \boldsymbol{z}_{i,k}^\dagger \tag{6}$$

$$\begin{aligned} \max_{\boldsymbol{R}_i} f_{0,i}\left(\boldsymbol{Z}_i\right) &= \left(\frac{K+1}{\pi e}\right)^{(K+1)N} \\ &\times \frac{1}{\det^{K+1}\left(\boldsymbol{S}_i\right)} \frac{1}{\left(1 + \boldsymbol{z}_i^\dagger \boldsymbol{S}_i^{-1} \boldsymbol{z}_i\right)^{K+1}} \end{aligned}$$

for $i \in \mathcal{N}_{\mathcal{R}} \setminus \mathcal{N}_{\mathcal{R}1}$ and

$$\begin{aligned} \max_{\boldsymbol{u}_i} \max_{\boldsymbol{R}_i} f_{0,i}\left(\boldsymbol{Z}_i\right) &= \left(\frac{K+1}{\pi e}\right)^{(K+1)N} \\ &\times \frac{1}{\det^{K+1}\left(\boldsymbol{S}_i' - \boldsymbol{w}_i \boldsymbol{w}_i^\dagger\right)} \end{aligned}$$

for $i \in \mathcal{N}_{\mathcal{R}1}$ with

$$\boldsymbol{w}_i = \boldsymbol{z}_i - \boldsymbol{v}_i \frac{\boldsymbol{v}_i^\dagger \boldsymbol{S}_i'^{-1} \boldsymbol{z}_i}{\boldsymbol{v}_i^\dagger \boldsymbol{S}_i'^{-1} \boldsymbol{v}_i}$$

and $\boldsymbol{S}_i' = \boldsymbol{S}_i + \boldsymbol{z}_i \boldsymbol{z}_i^\dagger = \sum_{k=1}^{K} \boldsymbol{z}_{i,k} \boldsymbol{z}_{i,k}^\dagger + \boldsymbol{z}_i \boldsymbol{z}_i^\dagger$. It turns out that the GLRT for the case at hand is given by

$$\prod_{i \in \mathcal{N}_{\mathcal{R}1}} \frac{\det\left(\boldsymbol{S}_i' - \boldsymbol{w}_i \boldsymbol{w}_i^\dagger\right)}{\det\left(\boldsymbol{S}_i\right) \left(1 + \boldsymbol{z}_i^\dagger \boldsymbol{S}_i^{-1} \boldsymbol{z}_i - \frac{|\boldsymbol{z}_i^\dagger \boldsymbol{S}_i^{-1} \boldsymbol{v}_i|^2}{\boldsymbol{v}_i^\dagger \boldsymbol{S}_i^{-1} \boldsymbol{v}_i}\right)} \times \prod_{i \in \mathcal{N}_{\mathcal{R}} \setminus \mathcal{N}_{\mathcal{R}1}} \frac{1 + \boldsymbol{z}_i^\dagger \boldsymbol{S}_i^{-1} \boldsymbol{z}_i}{1 + \boldsymbol{z}_i^\dagger \boldsymbol{S}_i^{-1} \boldsymbol{z}_i - \frac{|\boldsymbol{z}_i^\dagger \boldsymbol{S}_i^{-1} \boldsymbol{v}_i|^2}{\boldsymbol{v}_i^\dagger \boldsymbol{S}_i^{-1} \boldsymbol{v}_i}} \underset{H_0}{\overset{H_1}{\gtrless}} T \tag{7}$$

where T denotes a proper modification of the original threshold. If, instead, $\mathcal{N}_{\mathcal{R}1}$ is not known, but for its cardinality, r say, it turns out that the GLRT can be written as

$$\min_{\mathcal{N}_{\mathcal{R}1}} \prod_{i\in\mathcal{N}_{\mathcal{R}1}} \frac{\det\left(\boldsymbol{S}_i' - \boldsymbol{w}_i\boldsymbol{w}_i^\dagger\right)}{\det\left(\boldsymbol{S}_i\right)\left(1+\boldsymbol{z}_i^\dagger\boldsymbol{S}_i^{-1}\boldsymbol{z}_i - \dfrac{|\boldsymbol{z}_i^\dagger\boldsymbol{S}_i^{-1}\boldsymbol{v}_i|^2}{\boldsymbol{v}_i^\dagger\boldsymbol{S}_i^{-1}\boldsymbol{v}_i}\right)}$$
$$\times \prod_{i\in\mathcal{N}_{\mathcal{R}}\setminus\mathcal{N}_{\mathcal{R}1}} \frac{1+\boldsymbol{z}_i^\dagger\boldsymbol{S}_i^{-1}\boldsymbol{z}_i}{1+\boldsymbol{z}_i^\dagger\boldsymbol{S}_i^{-1}\boldsymbol{z}_i - \dfrac{|\boldsymbol{z}_i^\dagger\boldsymbol{S}_i^{-1}\boldsymbol{v}_i|^2}{\boldsymbol{v}_i^\dagger\boldsymbol{S}_i^{-1}\boldsymbol{v}_i}} \underset{H_0}{\overset{H_1}{\gtrless}} T \qquad (8)$$

where T is a threshold to be set according to the desired P_{fa}. A few remarks are now in order. First, observe that the detector is (up to the minimization over $\mathcal{N}_{\mathcal{R}1}$) the product of statistics equivalent to the well-known statistic of Kelly's detector, for $i\in\mathcal{N}_{\mathcal{R}}\setminus\mathcal{N}_{\mathcal{R}1}$, and to the W-ABORT, for $i\in\mathcal{N}_{\mathcal{R}1}$. Second, minimization over $\mathcal{N}_{\mathcal{R}1}$ cannot be conducted in closed form, thus limiting the feasibility of the detector for large values of N_R. However, to deal with an unknown $\mathcal{N}_{\mathcal{R}1}$, an ad hoc solution, consisting of the cascade of two stages, can also be conceived. The first stage is made by N_R classifiers: the ith classifier processes data collected by the ith radar to determine if the received signal contains an ECM signal, as shown in [15]. It relies on two detectors: an AMF [24] that is used to discriminate between the noise-only hypothesis and the alternative that a structured signal is present; in case of detection, a Kelly's detector is aimed at discriminating between mainlobe and sidelobe signals. The second stage is the GLRT for known I_i, fed by data collected by the overall network and by the output of the classifiers. Denoting by $\hat{I}_i$ the output of the ith classifier, where $\hat{I}_i = 1$ if the classifier has decided for the presence of an ECM signal ($\hat{I}_i = 0$ otherwise), the second stage ad hoc GLRT is obviously obtained from equation (7) by replacing $\mathcal{N}_{\mathcal{R}1}$ with the set of integers indexing the $\hat{I}_i$ that are equal to one. The overall ad hoc detector will be referred to as two stage network W-ABORT (2S-N-W-ABORT).

B. A GLRT for random I_i

Herein we model the I_is as rvs. More precisely, we assume that $I_1,\ldots,I_{N_R}$ are iid Bernoulli rvs, $I_i\sim\mathcal{B}(1,p)$, and, in addition, suppose that the set $\{I_1,\ldots,I_{N_R}\}$ is independent of that of the noise terms. For the time being we assume that $p\in(0,1)$ is known. It follows that the pdf of $\boldsymbol{Z}_i$ is given by equation (3) under H_1 and by

$$\begin{aligned} f_{0,i}(\boldsymbol{Z}_i) &= \left[pf_i\left(\boldsymbol{z}_i-\boldsymbol{u}_i\right)+(1-p)f_i\left(\boldsymbol{z}_i\right)\right]\prod_{k=1}^{K} f_i\left(\boldsymbol{z}_{i,k}\right) \\ &= \frac{1}{\pi^N\det(\boldsymbol{R}_i)}\Big[p\mathrm{e}^{-\left(\boldsymbol{z}_i-\boldsymbol{u}_i\right)^\dagger\boldsymbol{R}_i^{-1}\left(\boldsymbol{z}_i-\boldsymbol{u}_i\right)} \\ &+ (1-p)\mathrm{e}^{-\boldsymbol{z}_i^\dagger\boldsymbol{R}_i^{-1}\boldsymbol{z}_i}\Big] \\ &\times \prod_{k=1}^{K}\frac{1}{\pi^N\det(\boldsymbol{R}_i)}\mathrm{e}^{-\boldsymbol{z}_{i,k}^\dagger\boldsymbol{R}_i^{-1}\boldsymbol{z}_{i,k}} \end{aligned}$$

under H_0. Then, the GLRT is

$$\prod_{i\in\mathcal{N}_{\mathcal{R}}}\frac{\max_{\boldsymbol{R}_i}\max_{x_i} f_{1,i}\left(\boldsymbol{Z}_i\right)}{\max_{\boldsymbol{R}_i}\max_{\boldsymbol{u}_i} f_{0,i}\left(\boldsymbol{Z}_i\right)} \underset{H_0}{\overset{H_1}{\gtrless}} T \qquad (9)$$

where T is a threshold to be set according to the desired P_{fa}.

The compressed likelihood under H_1 can be expressed in terms of the right-hand side of equation (5). As to the maximization of the pdf of the observables under H_0, it is possible to show, following the lead of [21], that

$$\begin{aligned} \max_{\boldsymbol{u}_i} f_{0,i}(\boldsymbol{Z}_i) &= \max_{\boldsymbol{u}_i}\left[pf_i\left(\boldsymbol{z}_i-\boldsymbol{u}_i\right)+(1-p)f_i\left(\boldsymbol{z}_i\right)\right] \\ &\times \prod_{k=1}^{K} f_i\left(\boldsymbol{z}_{i,k}\right) \qquad (10) \\ &= \frac{1}{\pi^N\det(\boldsymbol{R}_i)}\left[p\ \mathrm{e}^{-\frac{\left|\boldsymbol{z}_i^\dagger\boldsymbol{R}_i^{-1}\boldsymbol{v}_i\right|^2}{\boldsymbol{v}_i^\dagger\boldsymbol{R}_i^{-1}\boldsymbol{v}_i}}\right. \\ &+ \left.(1-p)\ \mathrm{e}^{-\boldsymbol{z}_i^\dagger\boldsymbol{R}_i^{-1}\boldsymbol{z}_i}\right] \\ &\times \prod_{k=1}^{K}\frac{1}{\pi^N\det(\boldsymbol{R}_i)}\mathrm{e}^{-\boldsymbol{z}_{i,k}^\dagger\boldsymbol{R}_i^{-1}\boldsymbol{z}_{i,k}} \\ &= \frac{\mathrm{e}^{-\mathrm{Tr}\left(\boldsymbol{R}_i^{-1}\boldsymbol{S}_i'\right)}}{\pi^{N(K+1)}\det^{K+1}(\boldsymbol{R}_i)}\left[pg(\boldsymbol{R}_i)+(1-p)\right] \end{aligned}$$

where $\mathrm{Tr}(\cdot)$ denotes the trace of the matrix argument,

$$g(\boldsymbol{R}_i) = \mathrm{e}^{\boldsymbol{z}_i^\dagger\boldsymbol{R}_i^{-1}\boldsymbol{z}_i - \frac{\left|\boldsymbol{z}_i^\dagger\boldsymbol{R}_i^{-1}\boldsymbol{v}_i\right|^2}{\boldsymbol{v}_i^\dagger\boldsymbol{R}_i^{-1}\boldsymbol{v}_i}}$$

(and $\boldsymbol{S}_i' = \boldsymbol{S}_i + \boldsymbol{z}_i\boldsymbol{z}_i^\dagger = \sum_{k=1}^K \boldsymbol{z}_{i,k}\boldsymbol{z}_{i,k}^\dagger + \boldsymbol{z}_i\boldsymbol{z}_i^\dagger$). Setting to zero the derivative with respect to $\boldsymbol{R}_i$ of the above partially-compressed likelihood yields

$$\begin{aligned} &\frac{\partial}{\partial\boldsymbol{R}_i}\ \frac{\mathrm{e}^{-\mathrm{Tr}\left(\boldsymbol{R}_i^{-1}\boldsymbol{S}_i'\right)}}{\det^{K+1}(\boldsymbol{R}_i)}\left[pg(\boldsymbol{R}_i)+(1-p)\right] \\ &= -(K+1)\frac{\mathrm{e}^{-\mathrm{Tr}\left(\boldsymbol{R}_i^{-1}\boldsymbol{S}_i'\right)}}{\det^{K+1}(\boldsymbol{R}_i)}\left[pg(\boldsymbol{R}_i)+(1-p)\right]\boldsymbol{R}_i^{-1} \\ &+ \frac{\mathrm{e}^{-\mathrm{Tr}\left(\boldsymbol{R}_i^{-1}\boldsymbol{S}_i'\right)}}{\det^{K+1}(\boldsymbol{R}_i)}\left[pg(\boldsymbol{R}_i)+(1-p)\right]\boldsymbol{R}_i^{-1}\boldsymbol{S}_i'\boldsymbol{R}_i^{-1} \\ &- \frac{\mathrm{e}^{-\mathrm{Tr}\left(\boldsymbol{R}_i^{-1}\boldsymbol{S}_i'\right)}}{\det^{K+1}(\boldsymbol{R}_i)}pg(\boldsymbol{R}_i)\boldsymbol{R}_i^{-1}\left(\boldsymbol{z}_i - \frac{\boldsymbol{v}_i^\dagger\boldsymbol{R}_i^{-1}\boldsymbol{z}_i}{\boldsymbol{v}_i^\dagger\boldsymbol{R}_i^{-1}\boldsymbol{v}_i}\boldsymbol{v}_i\right) \\ &\times \left(\boldsymbol{z}_i - \frac{\boldsymbol{v}_i^\dagger\boldsymbol{R}_i^{-1}\boldsymbol{z}_i}{\boldsymbol{v}_i^\dagger\boldsymbol{R}_i^{-1}\boldsymbol{v}_i}\boldsymbol{v}_i\right)^\dagger\boldsymbol{R}_i^{-1} = 0\ . \end{aligned}$$

Letting

$$b_i(\boldsymbol{R}_i) = \frac{\boldsymbol{v}_i^\dagger\boldsymbol{R}_i^{-1}\boldsymbol{z}_i}{\boldsymbol{v}_i^\dagger\boldsymbol{R}_i^{-1}\boldsymbol{v}_i}$$

the previous equation can be re-written as

$$
\begin{aligned}
\frac{\partial}{\partial \boldsymbol{R}_i} \quad & \frac{\mathrm{e}^{-\mathrm{Tr}\left(\boldsymbol{R}_i^{-1}\boldsymbol{S}_i'\right)}}{\det^{K+1}(\boldsymbol{R}_i)} \left[pg(\boldsymbol{R}_i) + (1-p)\right] \\
= \quad & -(K+1)\frac{\mathrm{e}^{-\mathrm{Tr}\left(\boldsymbol{R}_i^{-1}\boldsymbol{S}_i'\right)}}{\det^{K+1}(\boldsymbol{R}_i)} \left[pg(\boldsymbol{R}_i) + (1-p)\right] \boldsymbol{R}_i^{-1} \\
+ \quad & \frac{\mathrm{e}^{-\mathrm{Tr}\left(\boldsymbol{R}_i^{-1}\boldsymbol{S}_i'\right)}}{\det^{K+1}(\boldsymbol{R}_i)} \left[pg(\boldsymbol{R}_i) + (1-p)\right] \boldsymbol{R}_i^{-1}\boldsymbol{S}_i'\boldsymbol{R}_i^{-1} \\
- \quad & \frac{\mathrm{e}^{-\mathrm{Tr}\left(\boldsymbol{R}_i^{-1}\boldsymbol{S}_i'\right)}}{\det^{K+1}(\boldsymbol{R}_i)} pg(\boldsymbol{R}_i)\boldsymbol{R}_i^{-1} \\
\times \quad & \left(\boldsymbol{z}_i - b_i(\boldsymbol{R}_i)\boldsymbol{v}_i\right)\left(\boldsymbol{z}_i - b_i(\boldsymbol{R}_i)\boldsymbol{v}_i\right)^{\dagger} \boldsymbol{R}_i^{-1} = 0\,. \quad (11)
\end{aligned}
$$

It turns out that stationary points must solve the following equation

$$
\begin{aligned}
(K+1)\boldsymbol{R}_i \quad = \quad & \boldsymbol{S}_i' - \frac{pg(\boldsymbol{R}_i)}{pg(\boldsymbol{R}_i) + (1-p)} \\
\times \quad & \left(\boldsymbol{z}_i - b_i(\boldsymbol{R}_i)\boldsymbol{v}_i\right)\left(\boldsymbol{z}_i - b_i(\boldsymbol{R}_i)\boldsymbol{v}_i\right)^{\dagger}
\end{aligned}
$$

or, otherwise stated, must have the following structure

$$
\boldsymbol{R}_i = \frac{1}{K+1}\left[\boldsymbol{S}_i' + a_i\boldsymbol{w}_i\boldsymbol{w}_i^{\dagger}\right], \quad a_i \in (-1,0), b_i \in \mathbb{C} \quad (12)
$$

where

$$
a_i = -\frac{pg(\boldsymbol{R}_i)}{pg(\boldsymbol{R}_i) + (1-p)}
$$

and

$$
\boldsymbol{w}_i = \boldsymbol{z}_i - b_i(\boldsymbol{R}_i)\boldsymbol{v}_i.
$$

The following theorem shows how to compute a_i and b_i.

Theorem 1: The solutions of equation (11) have the form of the right-hand side of (12) with

$$
b_i = \frac{\boldsymbol{v}_i^{\dagger}\boldsymbol{S}_i'^{-1}\boldsymbol{z}_i}{\boldsymbol{v}_i^{\dagger}\boldsymbol{S}_i'^{-1}\boldsymbol{v}_i} \quad (13)
$$

and $a_i \in (-1,0)$ computed by solving the following equation

$$
a_i = -\frac{1}{1 + \frac{1-p}{p}\,\mathrm{e}^{-(K+1)\frac{\boldsymbol{z}_i^{\dagger}\boldsymbol{S}_i'^{-1}\boldsymbol{z}_i - \frac{|\boldsymbol{v}_i^{\dagger}\boldsymbol{S}_i'^{-1}\boldsymbol{z}_i|^2}{\boldsymbol{v}_i^{\dagger}\boldsymbol{S}_i'^{-1}\boldsymbol{v}_i}}{1 + a_i\left(\boldsymbol{z}_i^{\dagger}\boldsymbol{S}_i'^{-1}\boldsymbol{z}_i - \frac{|\boldsymbol{v}_i^{\dagger}\boldsymbol{S}_i'^{-1}\boldsymbol{z}_i|^2}{\boldsymbol{v}_i^{\dagger}\boldsymbol{S}_i'^{-1}\boldsymbol{v}_i}\right)}}} \quad (14)
$$

Proof See Appendix A.

Thus, the ith factor of the compressed likelihood under H_0 is given by

$$
\begin{aligned}
\max_{\boldsymbol{R}_i,\boldsymbol{u}_i} f_{0,i}(\boldsymbol{Z}_i) \quad = \quad & \frac{\mathrm{e}^{-\mathrm{Tr}\left(\hat{\boldsymbol{R}}_{0,i}^{-1}\boldsymbol{S}_i'\right)}}{\pi^{N(K+1)}\det^{K+1}(\hat{\boldsymbol{R}}_{0,i})} \\
\times \quad & \left[pg(\hat{\boldsymbol{R}}_{0,i}) + (1-p)\right] \quad (15)
\end{aligned}
$$

with $\hat{\boldsymbol{R}}_{0,i}$ denoting the maximizer of the likelihood in the form of the right-hand side of equation (12), a_i and b_i, obtained, in turn, by Theorem 1. In particular, we compute the a_is by means of standard numerical root finding techniques.

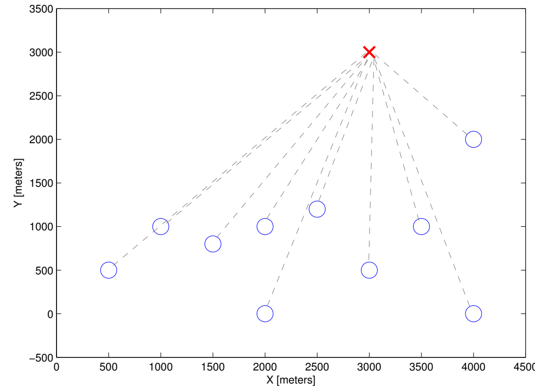

Fig. 1. Simulated scenario: circles indicate radar positions while the cross indicates the target position.

Then, the GLRT for the case at hand can be written as

$$
\prod_{i\in\mathcal{N}_{\mathcal{R}}} \frac{\frac{1}{\det^{K+1}(\boldsymbol{S}_i)}\frac{1}{\left(1+\boldsymbol{z}_i^{\dagger}\boldsymbol{S}_i^{-1}\boldsymbol{z}_i - \frac{|\boldsymbol{z}_i^{\dagger}\boldsymbol{S}_i^{-1}\boldsymbol{v}_i|^2}{\boldsymbol{v}_i^{\dagger}\boldsymbol{S}_i^{-1}\boldsymbol{v}_i}\right)^{K+1}}}{\frac{\mathrm{e}^{-\mathrm{Tr}\left(\hat{\boldsymbol{R}}_{0,i}^{-1}\boldsymbol{S}_i'\right)}}{\det^{K+1}\left(\hat{\boldsymbol{R}}_{0,i}\right)}\left[pg(\hat{\boldsymbol{R}}_{0,i}) + (1-p)\right]} \underset{H_0}{\overset{H_1}{\gtrless}} T
$$

It can also be recast as

$$
\prod_{i\in\mathcal{N}_{\mathcal{R}}} \Lambda_i\left(\boldsymbol{Z}_i\right) \underset{H_0}{\overset{H_1}{\gtrless}} T
$$

with

$$
\begin{aligned}
\Lambda_i\left(\boldsymbol{Z}_i\right) \quad = \quad & \frac{\frac{\mathrm{e}^{\mathrm{Tr}\left(\hat{\boldsymbol{R}}_{0,i}^{-1}\boldsymbol{S}_i'\right)}}{\det^{K+1}\left(\hat{\boldsymbol{R}}_{0,i}^{-1}\boldsymbol{S}_i\right)}}{\left[1+\boldsymbol{z}_i^{\dagger}\boldsymbol{S}_i^{-1}\boldsymbol{z}_i - \frac{|\boldsymbol{z}_i^{\dagger}\boldsymbol{S}_i^{-1}\boldsymbol{v}_i|^2}{\boldsymbol{v}_i^{\dagger}\boldsymbol{S}_i^{-1}\boldsymbol{v}_i}\right]^{K+1}} \\
\times \quad & \frac{1}{p\mathrm{e}^{\boldsymbol{z}_i^{\dagger}\hat{\boldsymbol{R}}_{0,i}^{-1}\boldsymbol{z}_i - \frac{\left|\boldsymbol{z}_i^{\dagger}\hat{\boldsymbol{R}}_{0,i}^{-1}\boldsymbol{v}_i\right|^2}{\boldsymbol{v}_i^{\dagger}\hat{\boldsymbol{R}}_{0,i}^{-1}\boldsymbol{v}_i}} + (1-p)}
\end{aligned}
$$

and will be referred to in the following as one stage network W-ABORT (1S-N-W-ABORT).

III. Performance analysis

The performance analysis is conducted by Monte Carlo simulation. To this end, we resort to $100/P_{fa}$ independent trials to evaluate the thresholds necessary to ensure a preassigned value of P_{fa} and to 10^4 independent trials to compute the probabilities to decide for H_1 under useful signal only (P_d), under ECM only, and under useful signal plus ECM.

We consider a scenario with $N_R = 10$ radars located as in Fig. 1, where circles indicate radar positions (and coordinates are expressed in meters). The radars have the same transmitted

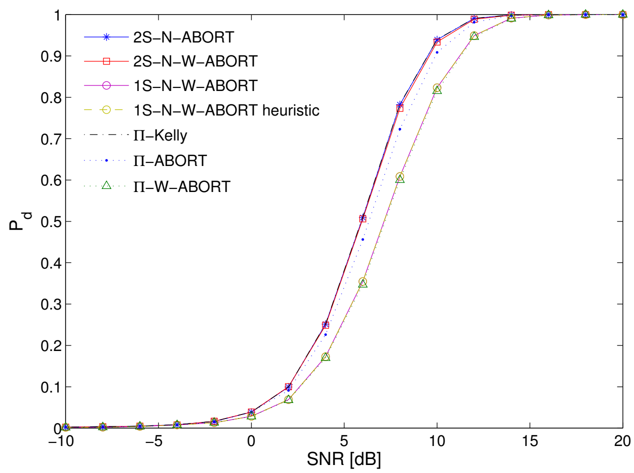

Fig. 2. P_d vs SNR in presence of target only (absence of ECM). $N = 4$ and $K = 8$.

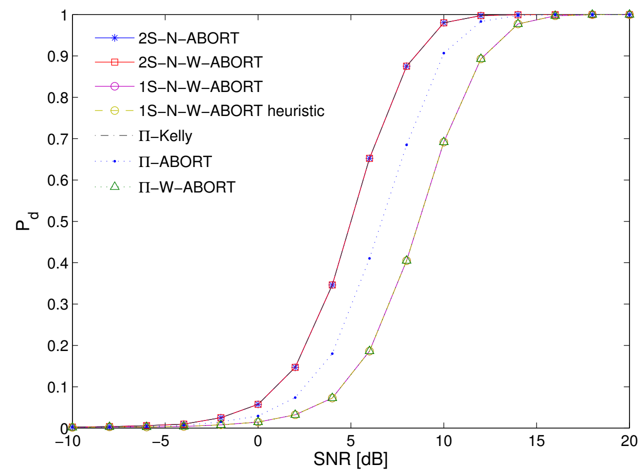

Fig. 3. P_d vs SNR in presence of target only (absence of ECM). $N = 16$ and $K = 32$.

power and antenna gain. Each radar has a different carrier frequency in a range of ± 250 MHz around 1 GHz, pulse repetition frequency equal to 5 kHz, $N_a = 1$ antennas. For each radar, the clutter is exponentially correlated with one-lag correlation coefficient equal to $\rho = 0.95$; more precisely, the (m,n)th entry of the matrix $\boldsymbol{R}_i$ is given by $r_{mn} = \rho^{|m-n|}$.

The cross indicates the target position, whose velocity modulus is constantly set to 300 m/s, while the direction is a rv uniformly distributed in $(0, 2\pi)$. Thus, at each iteration, the radial velocity of the target changes and so does the corresponding normalized Doppler frequency seen at each radar, ν_i say. The amplitudes of the target (i.e., the x_is) are generated as independent Rayleigh-distributed rvs. The signal-to-noise ratio at radar i (SNR$_i$) is defined as

$$\text{SNR}_i = E[x_i^2]\ \boldsymbol{v}_i^\dagger \boldsymbol{R}_i^{-1} \boldsymbol{v}_i.$$

Obviously,

$$\frac{\text{SNR}_i d_i^4}{\lambda_i^2} = \frac{\text{SNR}_j d_j^4}{\lambda_j^2}$$

where d_i is the distance of the ith radar to the target and λ_i the corresponding wavelength.

As regards the possible presence of a CRI, it is simulated as a signal aimed at deceiving the detector with a false target. To this end, it is simulated as a signal similar to $\boldsymbol{v}_i$, but for a mismatched Doppler frequency $\gamma\nu_i$ with γ a uniformly distributed rv in $(0, 1)$. The amplitude of the possible interferer at radar i is taken 100 times stronger than the root mean square value of the corresponding useful signal; it impinges on radar No. i with probability p and independent from radar to radar.

For comparison purposes we also consider three natural competitors, namely a "product of Kelly's statistics," referred to in the following as Π-Kelly, and given by

$$\prod_{i \in \mathcal{N}_\mathcal{R}} \frac{1 + \boldsymbol{z}_i^\dagger \boldsymbol{S}_i^{-1} \boldsymbol{z}_i}{1 + \boldsymbol{z}_i^\dagger \boldsymbol{S}_i^{-1} \boldsymbol{z}_i - \dfrac{|\boldsymbol{z}_i^\dagger \boldsymbol{S}_i^{-1} \boldsymbol{v}_i|^2}{\boldsymbol{v}_i^\dagger \boldsymbol{S}_i^{-1} \boldsymbol{v}_i}} \underset{H_0}{\overset{H_1}{\gtrless}} T$$

a "product of ABORT statistics," referred to in the following as Π-ABORT, namely (see also [25], [22])

$$\prod_{i \in \mathcal{N}_\mathcal{R}} \frac{1 + \dfrac{|\boldsymbol{z}_i^\dagger \boldsymbol{S}_i^{-1} \boldsymbol{v}_i|^2}{\boldsymbol{v}_i^\dagger \boldsymbol{S}_i^{-1} \boldsymbol{v}_i}}{1 + \boldsymbol{z}_i^\dagger \boldsymbol{S}_i^{-1} \boldsymbol{z}_i - \dfrac{|\boldsymbol{z}_i^\dagger \boldsymbol{S}_i^{-1} \boldsymbol{v}_i|^2}{\boldsymbol{v}_i^\dagger \boldsymbol{S}_i^{-1} \boldsymbol{v}_i}} \underset{H_0}{\overset{H_1}{\gtrless}} T$$

and a "product of W-ABORT statistics," referred to in the following as Π-W-ABORT, and given by

$$\prod_{i \in \mathcal{N}_\mathcal{R}} \frac{\det\left(\boldsymbol{S}_i' - \boldsymbol{w}_i \boldsymbol{w}_i^\dagger\right)}{\det\left(\boldsymbol{S}_i\right)\left(1 + \boldsymbol{z}_i^\dagger \boldsymbol{S}_i^{-1} \boldsymbol{z}_i - \dfrac{|\boldsymbol{z}_i^\dagger \boldsymbol{S}_i^{-1} \boldsymbol{v}_i|^2}{\boldsymbol{v}_i^\dagger \boldsymbol{S}_i^{-1} \boldsymbol{v}_i}\right)} \underset{H_0}{\overset{H_1}{\gtrless}} T$$

where

$$\boldsymbol{w}_i = \boldsymbol{z}_i - \boldsymbol{v}_i \frac{\boldsymbol{v}_i^\dagger \boldsymbol{S}_i'^{-1} \boldsymbol{z}_i}{\boldsymbol{v}_i^\dagger \boldsymbol{S}_i'^{-1} \boldsymbol{v}_i}.$$

In addition to the 2S-N-W-ABORT we also consider a two stage network detector implementing the plain ABORT idea to process data of radars that are supposed (as part of the decision process) under ECM; for this reason, it is referred to as 2S-N-ABORT. Finally, we consider a heuristic variant of the 1S-N-W-ABORT obtained letting $a_i = -1$, $i = 1, \ldots, N_R$, which is obviously less time-consuming than the 1S-N-W-ABORT.

The thresholds of the detectors are set to guarantee $P_{fa} = 10^{-3}$ by considering the noise-only distribution of the corresponding statistics. As to the implementation of the two-stage detectors (2S-N-ABORT and 2S-N-W-ABORT) we assume that for each classifier, the threshold of the AMF and that of the Kelly's detector are set to guarantee $P_{fa} = 10^{-3}$ separately.

Simulation results are reported in Figs. 2–10 as a function of SNR=SNR$_1$ where radar No. 1 is the one with coordinates $(3000, 500)$. More precisely, Figs. 2 and 3 plot P_d (namely the probability to decide H_1 in presence of target only) vs SNR of the proposed detectors (i.e., the 2S-N-W-ABORT, the 1S-N-W-ABORT, and the heuristic variant of the latter) and

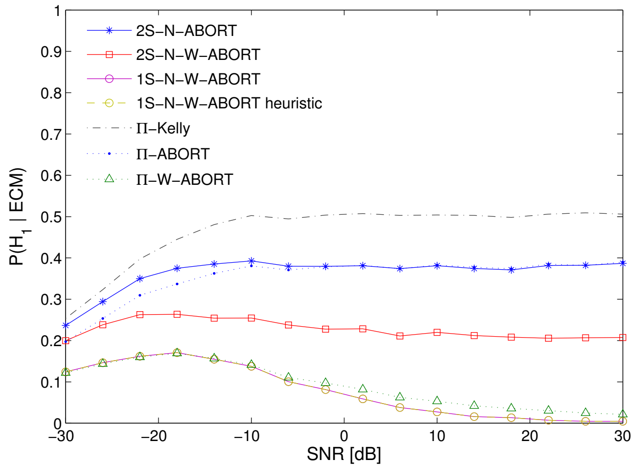

Fig. 4. Probability of (erroneously) detecting H_1 vs SNR in presence of ECM signals. $N = 4$, $K = 8$, and $p = 0.4$.

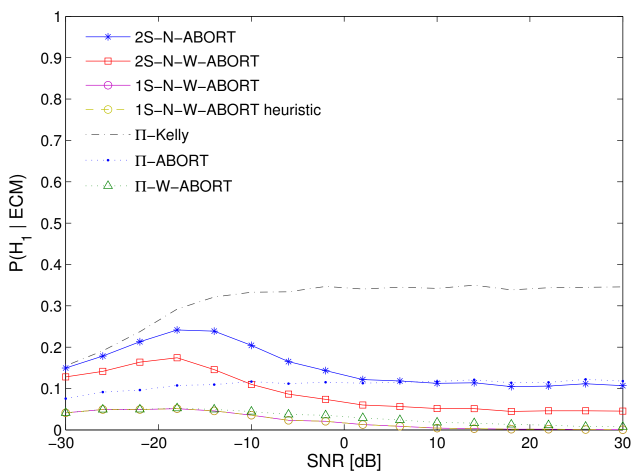

Fig. 5. Probability of (erroneously) detecting H_1 vs SNR in presence of ECM signals. $N = 16$, $K = 32$, and $p = 0.4$.

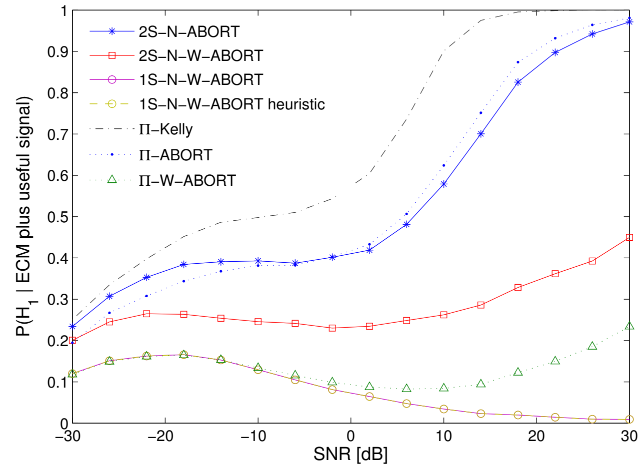

Fig. 6. Probability to detect H_1 vs SNR in presence of both target and ECM signals. $N = 4$, $K = 8$, and $p = 0.4$.

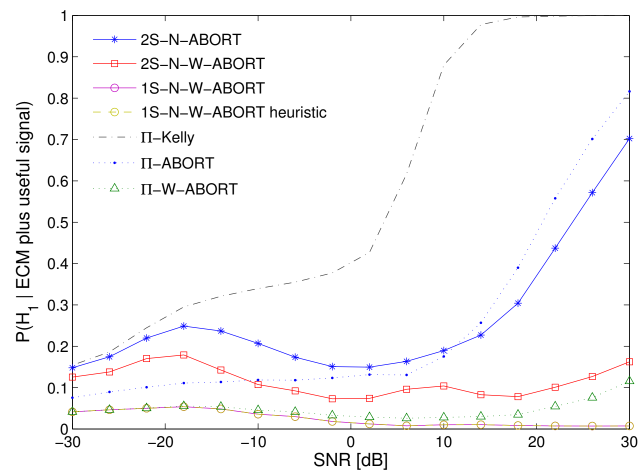

Fig. 7. Probability to detect H_1 vs SNR in presence of both target and ECM signals. $N = 16$, $K = 32$, and $p = 0.4$.

their competitors, while Figs. 4 and 5 refer to the presence of ECM signals only. Such figures show that the 2S-N-W-ABORT guarantees the detection power of the Π-Kelly, and better rejection capabilities than the Π-ABORT (and obviously of the Π-Kelly) for not too low SNR values. It is though less selective than the Π-W-ABORT and of both the 1S-N-W-ABORT and its heuristic variant. However, such more selective detectors are less powerful than the 2S-N-W-ABORT in presence of target only. In Figs. 6, 7, and 8 we plot the probability to detect the useful signal (H_1 hypothesis of the test) when both target and ECM signals are present. Figs. 6 and 7 refer to $p = 0.4$ while Fig. 8 assumes $p = 0.1$. It is apparent that the 1S-N-W-ABORT (and its heuristic variant), the 2S-N-W-ABORT, and the Π-W-ABORT are selective in that tend to reject a mix of target and ECM signals. In particular, the 1S-N-W-ABORT (and its heuristic variant as well) is the most effective one to reject the H_1 hypothesis in presence of ECM and possibly useful signal in the all range of SNR values. Notice also that the 1S-N-W-ABORT and its heuristic variant are practically equivalent in the considered instances.

We also conducted a preliminary analysis on the performance of the 1S-N-W-ABORT in order to quantify the influence of a possible mismatch between the actual (and unknown) value of p and the nominal one. For the ease of clarification, we distinguish in the following between the probability that a radar is under ECM, referred to as P(ECM), and the parameter p used in the design of the 1S-N-W-ABORT (also used for setting the threshold). In particular, in Figs. 9 and 10 we plot the performance of the 1S-N-W-ABORT designed assuming $p = 0.4$ in presence of ECM signals and ECM signals plus useful one, respectively. Results show that for P(ECM) $= 0.6$ and P(ECM) $= 0.9$ the detector designed for $p = 0.4$ returns performance very close to the performance for P(ECM) $= 0.4$ and, actually, very close to the performance that would have been obtained for $p = 0.6, 0.9$ (the corresponding curves are not included to avoid to burden too much the figures). The

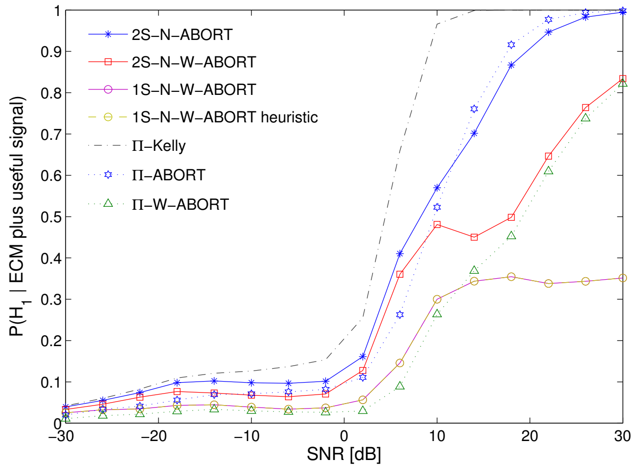

Fig. 8. Probability to detect H_1 vs SNR in presence of both target and ECM signals. $N = 16$, $K = 32$, and $p = 0.1$.

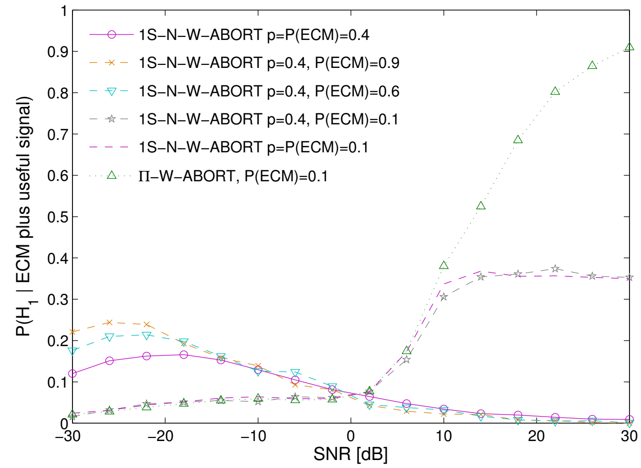

Fig. 10. Sensitivity analysis of the 1S-N-W-ABORT: probability to detect H_1 vs SNR in presence of both target and ECM signals. $N = 4$, $K = 8$.

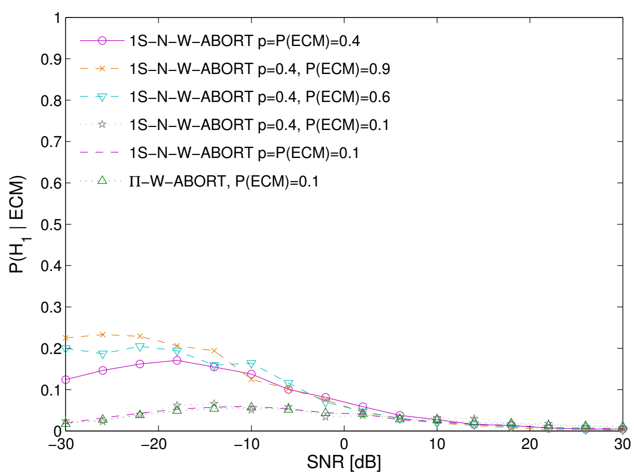

Fig. 9. Sensitivity analysis of the 1S-N-W-ABORT: probability of (erroneously) detecting H_1 vs SNR in presence of ECM signals. $N = 4$, $K = 8$.

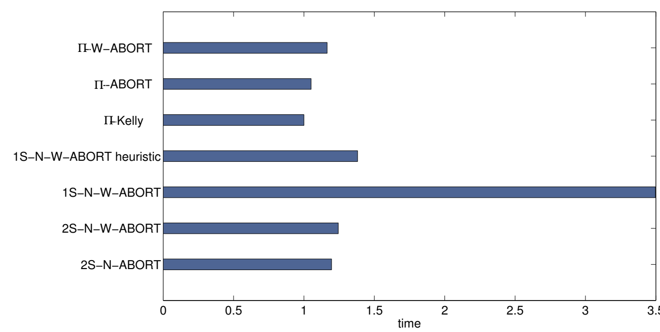

Fig. 11. Relative elapsed time, normalized to the fastest algorithm (Π-Kelly).

behavior of the detector is different for P(ECM) $= 0.1$: for this scenario the 1S-N-W-ABORT is less selective and, in fact, from Fig. 10, we see that the probability to choose H_1 (under ECM plus useful signal) increases and tends to about 0.35 for high SNR values. However, notice that the same is true for the 1S-N-W-ABORT designed for $p = 0.1$ and that, for P(ECM) $= 0.1$, the Π-W-ABORT is much less selective as shown in the same figure. This behavior can be easily explained observing that, for P(ECM) $= 0.1$, there is a non-negligible number of Monte Carlo runs where the ECM is absent; actually, for these cases, the probability to choose H_1, "under ECM plus useful signal," is P_d which, in turn, is close to one for high SNR values, as can be seen from Fig. 2. For this reason, in Fig. 10 and for P(ECM) $= 0.1$, we observe an increase of the probability to choose H_1 of both the 1S-N-W-ABORT and the Π-W-ABORT.

Finally, we have evaluated the relative computational time of the algorithms discussed above. Being the computational time linked to the complexity of the statistic, one can expect that the Π-Kelly is the fastest algorithm, while the 1S-N-W-ABORT is the slowest one due to the numerical resolution of equation (14). Notice that detectors involving the W-ABORT statistic require also the computation of $\boldsymbol{S}'$ and its inverse, and that the two-stage detectors require an additional detection task, though based on simple statistics.

The numerical results, reported in Fig. 11 in terms of relative elapsed time, are in agreement with the considerations above: in particular, the Π-ABORT and Π-W-ABORT are (slightly) more complex than the Π-Kelly, and the two-stage detectors immediately follow in the ranking; the 1S-N-W-ABORT has the greatest complexity, which however can be dramatically reduced avoiding the numerical resolution of equation (14), as indicated by the elapsed time of the heuristic variant with fixed $a_i = -1$.

IV. Conclusions

We have addressed adaptive detection of coherent signals backscattered by point-like targets in presence of disturbance and possible ECM signals, assuming a network of radars where for a given cell under test only a subset of the radars may receive ECM signals. The problem has been solved resorting to the GLRT and to ad hoc solutions. We considered two different instances: the subset of radars under ECM is deterministically given (but not necessarily known) or each radar is under ECM with a given probability. For the first case a two-stage architecture has been proposed: the first stage is aimed at detecting the radars that are actually under ECM; the second stage jointly processes the collected signals according to a GLRT strategy that "enhances the selectivity of the radars under ECM". For the second case we have designed the GLRT and also considered a heuristic variant. The performance analysis shows that the proposed solutions are effective in presence of ECM systems in that allow to reject the CRI while ensuring satisfactory performance in presence of useful signal only; in particular, it is possible to choose one of the proposed detectors according to the desired trade-off between selectivity and detection capabilities. Due to the terrific rejection capabilities of both the 1S-N-W-ABORT and its heuristic variant, it might be worth investigating the performance of a Π-Kelly (or even a more robust stage) cascaded by the proposed heuristic detector (due to its simplicity) to classify more accurately the following hypotheses: noise only, signal only, ECM (possibly plus a useful signal).

Finally, it is worth remarking that the increase in computational complexity of the proposed detectors compared to the competitors is very contained except for the 1S-N-W-ABORT, whose statistic requires a numerical rooting procedure. Simulations suggest that a great improvement might be obtained by means of a closed-form (approximate) solution, a point which is part of our ongoing work.

APPENDIX A
PROOF OF THEOREM 1

In the following we get rid of the index i.

By the matrix inversion lemma, we have that

$$\begin{aligned}
\boldsymbol{R}^{-1} &= (K+1)\left(\boldsymbol{S}' + a\boldsymbol{w}\boldsymbol{w}^\dagger\right)^{-1} \\
&= \frac{K+1}{a}\left(\frac{\boldsymbol{S}'}{a} + \boldsymbol{w}\boldsymbol{w}^\dagger\right)^{-1} \\
&= \frac{K+1}{a}\left(a\boldsymbol{S}'^{-1} - \frac{a^2\boldsymbol{S}'^{-1}\boldsymbol{w}\boldsymbol{w}^\dagger\boldsymbol{S}'^{-1}}{1+a\boldsymbol{w}^\dagger\boldsymbol{S}'^{-1}\boldsymbol{w}}\right) \\
&= (K+1)\left(\boldsymbol{S}'^{-1} - \frac{a\boldsymbol{S}'^{-1}\boldsymbol{w}\boldsymbol{w}^\dagger\boldsymbol{S}'^{-1}}{1+a\boldsymbol{w}^\dagger\boldsymbol{S}'^{-1}\boldsymbol{w}}\right)
\end{aligned}$$

and, hence, also that

$$\boldsymbol{z}^\dagger\boldsymbol{R}^{-1}\boldsymbol{z} = (K+1)\left(\boldsymbol{z}^\dagger\boldsymbol{S}'^{-1}\boldsymbol{z} - a\frac{|\boldsymbol{z}^\dagger\boldsymbol{S}'^{-1}\boldsymbol{w}|^2}{1+a\boldsymbol{w}^\dagger\boldsymbol{S}'^{-1}\boldsymbol{w}}\right)$$

$$\boldsymbol{v}^\dagger\boldsymbol{R}^{-1}\boldsymbol{z} = (K+1)\left(\boldsymbol{v}^\dagger\boldsymbol{S}'^{-1}\boldsymbol{z} - \frac{a\boldsymbol{v}^\dagger\boldsymbol{S}'^{-1}\boldsymbol{w}\boldsymbol{w}^\dagger\boldsymbol{S}'^{-1}\boldsymbol{z}}{1+a\boldsymbol{w}^\dagger\boldsymbol{S}'^{-1}\boldsymbol{w}}\right)$$

and

$$\boldsymbol{v}^\dagger\boldsymbol{R}^{-1}\boldsymbol{v} = (K+1)\left(\boldsymbol{v}^\dagger\boldsymbol{S}'^{-1}\boldsymbol{v} - a\frac{|\boldsymbol{v}^\dagger\boldsymbol{S}'^{-1}\boldsymbol{w}|^2}{1+a\boldsymbol{w}^\dagger\boldsymbol{S}'^{-1}\boldsymbol{w}}\right).$$

It turns out that

$$b = c/d \tag{16}$$

with

$$\begin{aligned}
c &= \boldsymbol{v}^\dagger\boldsymbol{S}'^{-1}\boldsymbol{z} \\
&+ a\left(\boldsymbol{v}^\dagger\boldsymbol{S}'^{-1}\boldsymbol{z}\ \boldsymbol{w}^\dagger\boldsymbol{S}'^{-1}\boldsymbol{w} - \boldsymbol{v}^\dagger\boldsymbol{S}'^{-1}\boldsymbol{w}\ \boldsymbol{w}^\dagger\boldsymbol{S}'^{-1}\boldsymbol{z}\right)
\end{aligned}$$

and

$$d = \boldsymbol{v}^\dagger\boldsymbol{S}'^{-1}\boldsymbol{v} + a\left(\boldsymbol{v}^\dagger\boldsymbol{S}'^{-1}\boldsymbol{v}\ \boldsymbol{w}^\dagger\boldsymbol{S}'^{-1}\boldsymbol{w} - |\boldsymbol{v}^\dagger\boldsymbol{S}'^{-1}\boldsymbol{w}|^2\right).$$

Moreover, we observe that

$$\begin{aligned}
\boldsymbol{w}^\dagger\boldsymbol{S}'^{-1}\boldsymbol{w} &= (\boldsymbol{z}-b\boldsymbol{v})^\dagger\boldsymbol{S}'^{-1}(\boldsymbol{z}-b\boldsymbol{v}) \\
&= \boldsymbol{z}^\dagger\boldsymbol{S}'^{-1}\boldsymbol{z} + |b|^2\boldsymbol{v}^\dagger\boldsymbol{S}'^{-1}\boldsymbol{v} \\
&- 2\mathbb{R}\left\{b\boldsymbol{z}^\dagger\boldsymbol{S}'^{-1}\boldsymbol{v}\right\},
\end{aligned} \tag{17}$$

$$\boldsymbol{v}^\dagger\boldsymbol{S}'^{-1}\boldsymbol{w} = \boldsymbol{v}^\dagger\boldsymbol{S}'^{-1}(\boldsymbol{z}-b\boldsymbol{v}) = \boldsymbol{v}^\dagger\boldsymbol{S}'^{-1}\boldsymbol{z} - b\boldsymbol{v}^\dagger\boldsymbol{S}'^{-1}\boldsymbol{v},$$

$$\begin{aligned}
\boldsymbol{w}^\dagger\boldsymbol{S}'^{-1}\boldsymbol{z} &= (\boldsymbol{z}-b\boldsymbol{v})^\dagger\boldsymbol{S}'^{-1}\boldsymbol{z} \\
&= \boldsymbol{z}^\dagger\boldsymbol{S}'^{-1}\boldsymbol{z} - \bar{b}\boldsymbol{v}^\dagger\boldsymbol{S}'^{-1}\boldsymbol{z},
\end{aligned} \tag{18}$$

$$\begin{aligned}
\boldsymbol{v}^\dagger\boldsymbol{S}'^{-1}\boldsymbol{w}\boldsymbol{w}^\dagger\boldsymbol{S}'^{-1}\boldsymbol{z} &= \left(\boldsymbol{v}^\dagger\boldsymbol{S}'^{-1}\boldsymbol{z} - b\boldsymbol{v}^\dagger\boldsymbol{S}'^{-1}\boldsymbol{v}\right) \\
&\times \left(\boldsymbol{z}^\dagger\boldsymbol{S}'^{-1}\boldsymbol{z} - \bar{b}\boldsymbol{v}^\dagger\boldsymbol{S}'^{-1}\boldsymbol{z}\right) \\
&= \boldsymbol{v}^\dagger\boldsymbol{S}'^{-1}\boldsymbol{z}\boldsymbol{z}^\dagger\boldsymbol{S}'^{-1}\boldsymbol{z} \\
&+ |b|^2\boldsymbol{v}^\dagger\boldsymbol{S}'^{-1}\boldsymbol{v}\boldsymbol{v}^\dagger\boldsymbol{S}'^{-1}\boldsymbol{z} \\
&- b\boldsymbol{v}^\dagger\boldsymbol{S}'^{-1}\boldsymbol{v}\boldsymbol{z}^\dagger\boldsymbol{S}'^{-1}\boldsymbol{z} \\
&- \bar{b}\left(\boldsymbol{v}^\dagger\boldsymbol{S}'^{-1}\boldsymbol{z}\right)^2,
\end{aligned}$$

and

$$\begin{aligned}
|\boldsymbol{v}^\dagger\boldsymbol{S}'^{-1}\boldsymbol{w}|^2 &= |\boldsymbol{v}^\dagger\boldsymbol{S}'^{-1}\boldsymbol{z} - b\boldsymbol{v}^\dagger\boldsymbol{S}'^{-1}\boldsymbol{v}|^2 \\
&= \left(\boldsymbol{v}^\dagger\boldsymbol{S}'^{-1}\boldsymbol{z} - b\boldsymbol{v}^\dagger\boldsymbol{S}'^{-1}\boldsymbol{v}\right) \\
&\times \left(\boldsymbol{z}^\dagger\boldsymbol{S}'^{-1}\boldsymbol{v} - \bar{b}\boldsymbol{v}^\dagger\boldsymbol{S}'^{-1}\boldsymbol{v}\right) \\
&= |\boldsymbol{v}^\dagger\boldsymbol{S}'^{-1}\boldsymbol{z}|^2 + |b|^2\left(\boldsymbol{v}^\dagger\boldsymbol{S}'^{-1}\boldsymbol{v}\right)^2 \\
&- 2\mathbb{R}\left\{b\boldsymbol{v}^\dagger\boldsymbol{S}'^{-1}\boldsymbol{v}\boldsymbol{z}^\dagger\boldsymbol{S}'^{-1}\boldsymbol{v}\right\}.
\end{aligned}$$

Moreover,

$$\begin{aligned}
c' &= \boldsymbol{v}^\dagger\boldsymbol{S}'^{-1}\boldsymbol{z}\ \boldsymbol{w}^\dagger\boldsymbol{S}'^{-1}\boldsymbol{w} - \boldsymbol{v}^\dagger\boldsymbol{S}'^{-1}\boldsymbol{w}\ \boldsymbol{w}^\dagger\boldsymbol{S}'^{-1}\boldsymbol{z} \\
&= b\left(\boldsymbol{v}^\dagger\boldsymbol{S}'^{-1}\boldsymbol{v}\boldsymbol{z}^\dagger\boldsymbol{S}'^{-1}\boldsymbol{z} - |\boldsymbol{v}^\dagger\boldsymbol{S}'^{-1}\boldsymbol{z}|^2\right)
\end{aligned} \tag{19}$$

and

$$\begin{aligned}
d' &= \boldsymbol{v}^\dagger\boldsymbol{S}'^{-1}\boldsymbol{v}\ \boldsymbol{w}^\dagger\boldsymbol{S}'^{-1}\boldsymbol{w} - |\boldsymbol{v}^\dagger\boldsymbol{S}'^{-1}\boldsymbol{w}|^2 \\
&= \boldsymbol{v}^\dagger\boldsymbol{S}'^{-1}\boldsymbol{v}\boldsymbol{z}^\dagger\boldsymbol{S}'^{-1}\boldsymbol{z} - |\boldsymbol{v}^\dagger\boldsymbol{S}'^{-1}\boldsymbol{z}|^2.
\end{aligned} \tag{20}$$

It follows that equation (16) can be re-written as

$$b = \frac{\boldsymbol{v}^\dagger\boldsymbol{S}'^{-1}\boldsymbol{z} + ac'}{\boldsymbol{v}^\dagger\boldsymbol{S}'^{-1}\boldsymbol{v} + ad'} \tag{21}$$

that finally yields

$$b = \frac{\boldsymbol{v}^\dagger\boldsymbol{S}'^{-1}\boldsymbol{z}}{\boldsymbol{v}^\dagger\boldsymbol{S}'^{-1}\boldsymbol{v}}. \tag{22}$$

On the other hand, in order to compute a we start with

$$\begin{aligned}
\tfrac{1}{K+1} \quad \ln\left[g(\boldsymbol{R})\right] &= \frac{1}{K+1}\left(\boldsymbol{z}^\dagger \boldsymbol{R}^{-1}\boldsymbol{z} - \frac{\left|\boldsymbol{z}^\dagger \boldsymbol{R}^{-1}\boldsymbol{v}\right|^2}{\boldsymbol{v}^\dagger \boldsymbol{R}^{-1}\boldsymbol{v}}\right)\\
&= \left(\boldsymbol{z}^\dagger \boldsymbol{S}'^{-1}\boldsymbol{z} - a\frac{|\boldsymbol{z}^\dagger \boldsymbol{S}'^{-1}\boldsymbol{w}|^2}{1+a\boldsymbol{w}^\dagger \boldsymbol{S}'^{-1}\boldsymbol{w}}\right)\\
&- \frac{\left|\left(\boldsymbol{v}^\dagger \boldsymbol{S}'^{-1}\boldsymbol{z} - \frac{a\boldsymbol{v}^\dagger \boldsymbol{S}'^{-1}\boldsymbol{w}\boldsymbol{w}^\dagger \boldsymbol{S}'^{-1}\boldsymbol{z}}{1+a\boldsymbol{w}^\dagger \boldsymbol{S}'^{-1}\boldsymbol{w}}\right)\right|^2}{\left(\boldsymbol{v}^\dagger \boldsymbol{S}'^{-1}\boldsymbol{v} - a\frac{|\boldsymbol{v}^\dagger \boldsymbol{S}'^{-1}\boldsymbol{w}|^2}{1+a\boldsymbol{w}^\dagger \boldsymbol{S}'^{-1}\boldsymbol{w}}\right)}\\
&= \frac{\boldsymbol{z}^\dagger \boldsymbol{S}'^{-1}\boldsymbol{z} + ae}{1+a\boldsymbol{w}^\dagger \boldsymbol{S}'^{-1}\boldsymbol{w}} - \frac{\frac{\left|\boldsymbol{v}^\dagger \boldsymbol{S}'^{-1}\boldsymbol{z}+ac'\right|^2}{(1+a\boldsymbol{w}^\dagger \boldsymbol{S}'^{-1}\boldsymbol{w})^2}}{\frac{\boldsymbol{v}^\dagger \boldsymbol{S}'^{-1}\boldsymbol{v}+ad'}{1+a\boldsymbol{w}^\dagger \boldsymbol{S}'^{-1}\boldsymbol{w}}}\\
&= \frac{\boldsymbol{z}^\dagger \boldsymbol{S}'^{-1}\boldsymbol{z} + ae}{1+a\boldsymbol{w}^\dagger \boldsymbol{S}'^{-1}\boldsymbol{w}}\\
&- \frac{\left|\boldsymbol{v}^\dagger \boldsymbol{S}'^{-1}\boldsymbol{z}+ac'\right|^2}{(1+a\boldsymbol{w}^\dagger \boldsymbol{S}'^{-1}\boldsymbol{w})(\boldsymbol{v}^\dagger \boldsymbol{S}'^{-1}\boldsymbol{v}+ad')} \qquad (23)
\end{aligned}$$

where

$$e = \boldsymbol{z}^\dagger \boldsymbol{S}'^{-1}\boldsymbol{z}\boldsymbol{w}^\dagger \boldsymbol{S}'^{-1}\boldsymbol{w} - |\boldsymbol{z}^\dagger \boldsymbol{S}'^{-1}\boldsymbol{w}|^2.$$

Then, we observe that, plugging equation (22) into equations (17) and (18), yields

$$\begin{aligned}
\boldsymbol{w}^\dagger \boldsymbol{S}'^{-1}\boldsymbol{w} &= \boldsymbol{z}^\dagger \boldsymbol{S}'^{-1}\boldsymbol{z} + |b|^2\boldsymbol{v}^\dagger \boldsymbol{S}'^{-1}\boldsymbol{v}\\
&- 2\mathbb{R}\left\{b\boldsymbol{z}^\dagger \boldsymbol{S}'^{-1}\boldsymbol{v}\right\}\\
&= \boldsymbol{z}^\dagger \boldsymbol{S}'^{-1}\boldsymbol{z} - \frac{\left|\boldsymbol{v}^\dagger \boldsymbol{S}'^{-1}\boldsymbol{z}\right|^2}{\boldsymbol{v}^\dagger \boldsymbol{S}'^{-1}\boldsymbol{v}} \qquad (24)
\end{aligned}$$

and

$$\begin{aligned}
\boldsymbol{w}^\dagger \boldsymbol{S}'^{-1}\boldsymbol{z} &= \boldsymbol{z}^\dagger \boldsymbol{S}'^{-1}\boldsymbol{z} - \bar{b}\boldsymbol{v}^\dagger \boldsymbol{S}'^{-1}\boldsymbol{z}\\
&= \boldsymbol{z}^\dagger \boldsymbol{S}'^{-1}\boldsymbol{z} - \frac{\left|\boldsymbol{v}^\dagger \boldsymbol{S}'^{-1}\boldsymbol{z}\right|^2}{\boldsymbol{v}^\dagger \boldsymbol{S}'^{-1}\boldsymbol{v}},
\end{aligned}$$

hence,

$$\begin{aligned}
\left|\boldsymbol{w}^\dagger \boldsymbol{S}'^{-1}\boldsymbol{z}\right|^2 &= \left(\boldsymbol{z}^\dagger \boldsymbol{S}'^{-1}\boldsymbol{z}\right)^2 + \frac{\left|\boldsymbol{v}^\dagger \boldsymbol{S}'^{-1}\boldsymbol{z}\right|^4}{\left(\boldsymbol{v}^\dagger \boldsymbol{S}'^{-1}\boldsymbol{v}\right)^2}\\
&- 2\boldsymbol{z}^\dagger \boldsymbol{S}'^{-1}\boldsymbol{z}\frac{\left|\boldsymbol{v}^\dagger \boldsymbol{S}'^{-1}\boldsymbol{z}\right|^2}{\boldsymbol{v}^\dagger \boldsymbol{S}'^{-1}\boldsymbol{v}}.
\end{aligned}$$

It turns out that

$$\begin{aligned}
e &= \boldsymbol{z}^\dagger \boldsymbol{S}'^{-1}\boldsymbol{z}\left(\boldsymbol{z}^\dagger \boldsymbol{S}'^{-1}\boldsymbol{z} - \frac{\left|\boldsymbol{v}^\dagger \boldsymbol{S}'^{-1}\boldsymbol{z}\right|^2}{\boldsymbol{v}^\dagger \boldsymbol{S}'^{-1}\boldsymbol{v}}\right)\\
&- \left(\boldsymbol{z}^\dagger \boldsymbol{S}'^{-1}\boldsymbol{z}\right)^2 - \frac{\left|\boldsymbol{v}^\dagger \boldsymbol{S}'^{-1}\boldsymbol{z}\right|^4}{\left(\boldsymbol{v}^\dagger \boldsymbol{S}'^{-1}\boldsymbol{v}\right)^2}\\
&+ 2\boldsymbol{z}^\dagger \boldsymbol{S}'^{-1}\boldsymbol{z}\frac{\left|\boldsymbol{v}^\dagger \boldsymbol{S}'^{-1}\boldsymbol{z}\right|^2}{\boldsymbol{v}^\dagger \boldsymbol{S}'^{-1}\boldsymbol{v}}\\
&= \boldsymbol{z}^\dagger \boldsymbol{S}'^{-1}\boldsymbol{z}\frac{\left|\boldsymbol{v}^\dagger \boldsymbol{S}'^{-1}\boldsymbol{z}\right|^2}{\boldsymbol{v}^\dagger \boldsymbol{S}'^{-1}\boldsymbol{v}} - \frac{\left|\boldsymbol{v}^\dagger \boldsymbol{S}'^{-1}\boldsymbol{z}\right|^4}{\left(\boldsymbol{v}^\dagger \boldsymbol{S}'^{-1}\boldsymbol{v}\right)^2}\\
&= \frac{\left|\boldsymbol{v}^\dagger \boldsymbol{S}'^{-1}\boldsymbol{z}\right|^2}{\boldsymbol{v}^\dagger \boldsymbol{S}'^{-1}\boldsymbol{v}}\left(\boldsymbol{z}^\dagger \boldsymbol{S}'^{-1}\boldsymbol{z} - \frac{\left|\boldsymbol{v}^\dagger \boldsymbol{S}'^{-1}\boldsymbol{z}\right|^2}{\boldsymbol{v}^\dagger \boldsymbol{S}'^{-1}\boldsymbol{v}}\right). \qquad (25)
\end{aligned}$$

Then, plugging equation (25), together with equations (19), (20), and (24), into the right-most side of equation (23), returns after some algebra

$$\frac{\ln\left[g(\boldsymbol{R})\right]}{K+1} = \frac{\boldsymbol{z}^\dagger \boldsymbol{S}'^{-1}\boldsymbol{z} - \frac{|\boldsymbol{v}^\dagger \boldsymbol{S}'^{-1}\boldsymbol{z}|^2}{\boldsymbol{v}^\dagger \boldsymbol{S}'^{-1}\boldsymbol{v}}}{1+a\left(\boldsymbol{z}^\dagger \boldsymbol{S}'^{-1}\boldsymbol{z} - \frac{|\boldsymbol{v}^\dagger \boldsymbol{S}'^{-1}\boldsymbol{z}|^2}{\boldsymbol{v}^\dagger \boldsymbol{S}'^{-1}\boldsymbol{v}}\right)}. \qquad (26)$$

Finally, we observe that equation

$$-a = \frac{pg(\boldsymbol{R})}{pg(\boldsymbol{R}) + (1-p)}$$

can be re-cast as

$$a = -\frac{1}{1+\frac{1-p}{p}\frac{1}{g(\boldsymbol{R})}}$$

and that, by using equation (26), we get the equation for a in the statement of the theorem. **Q.E.D.**

REFERENCES

[1] A. Farina, "Electronic Counter-countermeasures," in *Radar Handbook*, 3rd ed., M. Skolnik (ed.) Chapter 24, McGraw-Hill, 2008.

[2] S. D. Berger, "Digital Radio Frequency Memory Linear Range Gate Stealer Spectrum," *IEEE Trans. Aerospace and Electronic Systems*, Vol. 39, No. 2, pp. 725-735, April 2003.

[3] M. Greco, F. Gini, and A. Farina, "Combined Effect of Phase and RGPO Delay Quantization on Jamming Signal Spectrum," *Proc. of IEEE International Radar Conference*, Arlington, VA, USA, 9-12 May 2005.

[4] G. De Vito, A. Farina, R. Sanzullo, and L. Timmoneri, "Comparison between two adaptive algorithms for cancellation of noise like and coherent repeater interference," *Proc. of International Symposium on Radar, IRS98*, Munich, Germany, 15-17 September 1998.

[5] A. Farina, L. Timmoneri, and R. Tosini, "Cascading SLB and SLC devices," *Signal Processing*, Vol. 45, No. 2, pp. 261-266, August 1995.

[6] S. Z. Kalson, "An adaptive array detector with mismatched signal rejection," *IEEE Trans. Aerospace and Electronic Systems*, Vol. 28, No. 1, pp. 195-207, January 1992.

[7] C. D. Richmond, "The Theoretical Performance of a Class of Space-Time Adaptive Detection and Training Strategies for Airborne Radar," *Proc. of 32nd Annual Asilomar Conference on Signals, Systems, and Computers*, Pacific Grove, CA, USA, 1-4 November 1998.

[8] N. B. Pulsone and M. A. Zatman, "A computationally-efficient two-step implementation of the GLRT," *IEEE Trans. Signal Processing*, Vol. 48, No. 3, pp. 609-616, March 2000.

[9] C. D. Richmond, "Performance of the adaptive sidelobe blanker detection algorithm in homogeneous clutter," *IEEE Trans. Signal Processing*, Vol. 48, No. 5, pp. 1235-1247, May 2000.

[10] C. D. Richmond, "Performance of a Class of Adaptive Detection Algorithms in Nonhomogeneous Environments," *IEEE Trans. Signal Processing*, Vol. 48, No. 5, pp. 1248-1262, May 2000.

[11] A. De Maio, "Robust adaptive radar detection in the presence of steering vector mismatches," *IEEE Trans. Aerospace and Electronic Systems*, Vol. 41, No. 4, pp. 1322-1337, October 2005.

[12] F. Bandiera, A. De Maio, and G. Ricci, "Adaptive CFAR Radar Detection With Conic Rejection," *IEEE Trans. Signal Processing*, Vol. 55, No. 6, pp. 2533-2541, June 2006.

[13] O. Besson, "Detection of a Signal in Linear Subspace with Bounded Mismatch," *IEEE Trans. Aerospace and Electronic Systems*, Vol. 42, No. 3, pp. 1131-1139, July 2006.

[14] A. De Maio, "Rao Test for Adaptive Detection in Gaussian Interference with Unknown Covariance Matrix," *IEEE Trans. Signal Processing*, Vol. 55, No. 7, pp. 3577-3584, July 2007.

[15] M. Greco, F. Gini, and A. Farina, "Radar Detection and Classification of Jamming Signals Belonging to a Cone Class," *IEEE Trans. Signal Processing*, Vol. 56, No. 5, pp. 1984-1993, May 2008.

[16] F. Bandiera, D. Orlando, and G. Ricci, "A Subspace-based Adaptive Sidelobe Blanker," *IEEE Trans. Signal Processing*, Vol. 56, No. 9, pp. 4141-4151, September 2008.

[17] F. Bandiera, O. Besson, D. Orlando, and G. Ricci, "An Improved Adaptive Sidelobe Blanker," *IEEE Trans. Signal Processing*, Vol. 56, No. 9, pp. 4152-4161, September 2008.
[18] F. Bandiera, D. Orlando, and G. Ricci, "Advanced radar detection schemes under mismatched signal models," *Synthesis Lectures on Signal Processing, Morgan & Claypool Publishers*, March 2009.
[19] F. Bandiera, A. Farina, D. Orlando, and G. Ricci, "Detection algorithms to discriminate between radar targets and ECM signals", *IEEE Trans. Signal Processing*, Vol. 58, No. 12, pp. 5984-5993, December 2010.
[20] S. Buzzi, M. Lops, L. Venturino, and M. Ferri, "Track-Before-Detect Procedures in a Multi-Target Environment," *IEEE Trans. Aerospace and Electronic Systems*, Vol. 44, No. 3, pp. 1135-1150, July 2008.
[21] F. Bandiera, O. Besson, and G. Ricci, "An ABORT-Like Detector With Improved Mismatched Signals Rejection Capabilities," *IEEE Trans. Signal Processing*, Vol. 56, No. 1, pp. 14-25, January 2008.
[22] A. Coluccia and G. Ricci, "A radar network based W-ABORT approach to counteract deceptive ECM signals," *Proc. of IEEE International Symposium on INnovations in Intelligent SysTems and Applications (INISTA)*, Alberobello, Italy, 23-25 June 2014.
[23] E. J. Kelly, "An Adaptive Detection Algorithm," *IEEE Trans. Aerospace and Electronic Systems*, Vol. 22, No. 2, pp. 115-127, March 1986.
[24] F. C. Robey, D. L. Fuhrman, E. J. Kelly, and R. Nitzberg, "A CFAR Adaptive Matched Filter Detector," *IEEE Trans. Aerospace and Electronic Systems*, Vol. 29, No. 1, pp. 208-216, January 1992.
[25] N. B. Pulsone and C. M. Rader, "Adaptive Beamformer Orthogonal Rejection Test," *IEEE Trans. Signal Processing*, Vol. 49, No. 3, pp. 521-529, March 2001.

Angelo Coluccia received the Eng. degree in Telecommunication Engineering (summa cum laude) in 2007 and the PhD degree in Information Engineering in 2011, both from the University of Salento, Lecce, Italy. Former researcher at Forschungszentrum Telekommunikation Wien, Vienna, since 2008 he has been engaged in research projects on traffic analysis, security and anomaly detection in operational cellular networks. He is currently Assistant Professor at the Dipartimento di Ingegneria dell'Innovazione, University of Salento, where he teaches the course of Telecommunication Systems. His research interests are signal processing, communications and wireless networks, in particular cooperative sensing/estimation approaches for localization and other (possibly distributed) applications.

Giuseppe Ricci was born in Naples, Italy, on February 15, 1964. He received the Dr. degree and the Ph.D. degree, both in Electronic Engineering, from the University of Naples "Federico II" in 1990 and 1994, respectively. Since 1995 he has been with the University of Salento (formerly University of Lecce) first as an Assistant Professor of Telecommunications and, since 2002, as a Professor. His research interests are in the field of statistical signal processing with emphasis on radar processing, localization algorithms, and CDMA systems. More precisely, he has focused on high-resolution radar clutter modeling, detection of radar signals in Gaussian and non-Gaussian disturbance, oil spill detection from SAR data, track-before-detect algorithms fed by space-time radar data, localization in wireless sensor networks, multiuser detection in overlay CDMA systems, and blind multiuser detection. He has held visiting positions at the University of Colorado at Boulder (CO, USA) in 1997-1998 and in April/May 2001, at the Colorado State University (CO, USA) in July/September 2003, March 2005, September 2009, and March 2011, at Ensica (Toulouse, France) in March 2006, and at the University of Connecticut (Storrs CT, USA) in September 2008.